Interdependence of climate, soil, and vegetation as constrained by the Budyko curve

Pierre Gentine,[1] Paolo D'Odorico,[2] Benjamin R. Lintner,[3] Gajan Sivandran,[4] and Guido Salvucci[5]

Received 8 August 2012; revised 6 September 2012; accepted 10 September 2012; published 9 October 2012.

[1] The Budyko curve is an empirical relation among evapotranspiration, potential evapotranspiration and precipitation observed across a variety of landscapes and biomes around the world. Using data from more than three hundred catchments and a simple water balance model, the Budyko curve is inverted to explore the ecohydrological controls of the soil water balance. Comparing the results across catchments reveals that aboveground transpiration efficiency and belowground rooting structure have adapted to the dryness index and the phase lag between peak seasonal radiation and precipitation. The vertical and/or lateral extent of the rooting zone exhibits a maximum in semi-arid catchments or when peak radiation and precipitation are out of phase. This demonstrates plant strategies in Mediterranean climates in order to cope with water stress: the deeper rooting structure buffers the phase difference between precipitation and radiation. Results from this study can be used to constrain land-surface parameterizations in ungauged basins or general circulation models. **Citation:** Gentine, P., P. D'Odorico, B. R. Lintner, G. Sivandran, and G. Salvucci (2012), Interdependence of climate, soil, and vegetation as constrained by the Budyko curve, *Geophys. Res. Lett.*, *39*, L19404, doi:10.1029/2012GL053492.

1. Introduction

[2] Observations of the annual surface water balance across the globe demonstrate tight and relatively simple dependence of evapotranspiration on the atmospheric water source (precipitation) and demand (potential evaporation). One of the main challenges in modern hydrology is to understand this observed similarity of the annual surface water budget across a wide and diverse range of catchments types [*Milly*, 1994]. The large number of parameters required by typical hydrologic models limits our capacity to comprehend and explain this insensitivity of the annual water budget to catchment characteristics. The hydrological parameters in land surface models are usually assumed to be independent, but in reality, soil, topography, vegetation and climate are intimately interconnected [*Dietrich and Perron*, 2006]. Such parameter interdependence could reduce the range and variability of model response, consistent with the observed similarity of evapotranspiration dependence on source and demand characteristics.

[3] The observed similarity led to the development of simplified analytical parameterizations of the annual water balance [*Schreiber*, 1904; *Ol'dekop*, 1911; *Budyko*, 1961]. Among such simplified approaches, *Budyko* [1961] introduced the most widely used framework to determine long-term catchment evapotranspiration as a function of the catchment aridity index, $\left[\bar{\phi}\right] = \left[\overline{E_p}\right]/[P]$, in which $\left[\overline{E_p}\right]$ is the climatological annual potential evaporation and $\left[\overline{P}\right]$ is the climatological annual precipitation (overbars denote yearly averages and brackets denote long-term climatological means, i.e., the ensemble mean across years). Climatological evapotranspiration is related to the aridity index using a semi-empirical model:

$$\frac{\left[\overline{ET}\right]}{\left[\overline{P}\right]} = \left(\left[\bar{\phi}\right]\tanh\left(\frac{1}{\left[\bar{\phi}\right]}\right)\left(1 - \exp\left(-\left[\bar{\phi}\right]\right)\right)\right)^{1/2}. \quad (1)$$

This relationship is known as the "Budyko curve". Budyko tested this relationship against annual *ET*, computed as the residual between measured precipitation and catchment streamflow *Q*, over more than 1200 medium-size catchments (area > 1000 km^2).

[4] Unfortunately, catchment hydrology still lacks a theory explaining this relatively simple behavior across catchments with diverse geographical, soil, climate and vegetation conditions. To address this gap in our understanding, the Budyko curve has received renewed attention in recent years [e.g., *Milly*, 1994; *Koster and Suarez*, 1999; *Zhang et al.*, 2008; *Milly and Dunne*, 2002; *Porporato et al.*, 2004; *Potter et al.*, 2005; *Donohue et al.*, 2007; *Yang et al.*, 2008; *Gerrits et al.*, 2009; *Sivapalan et al.*, 2011]. These studies have used simplified models of the surface and groundwater storage to investigate the robustness of the Budyko curve across seemingly very different catchments.

[5] *Horton* [1933] and, more recently, *Troch et al.* [2009], hypothesized that the "natural vegetation of a region tends to develop to utilize the largest proportion of the available soil moisture supplied by infiltration" and that the vegetation adapts to local climate variability. Similarly, *Eagleson* [1978a, 1978b, 1978c, 1982] and *Eagleson and Tellers* [1982] emphasized the role of vegetation as both a cause and consequence of the hydrologic cycle. Eagleson introduced a

[1]Earth and Environmental Engineering, Columbia University, New York, New York, USA.
[2]Department of Environmental Sciences, University of Virginia, Charlottesville, Virginia, USA.
[3]Department of Environmental Sciences, Rutgers, State University of New Jersey, New Brunswick, New Jersey, USA.
[4]Civil, Environmental, and Geodetic Engineering, Ohio State University, Columbus, Ohio, USA.
[5]Department of Earth Sciences and Department of Geography, Boston University, Boston, Massachusetts, USA.

Corresponding author: P. Gentine, Earth and Environmental Engineering, Columbia University, 500 W 120th St., New York, NY 10027, USA. (pg2328@columbia.edu)

0094-8276/12/2012GL053492

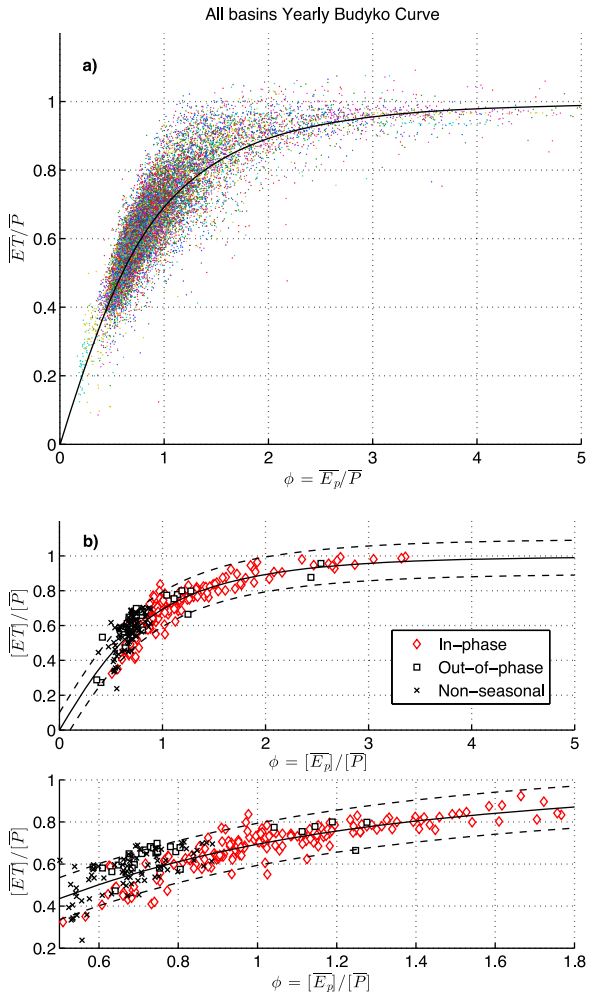

Figure 1. (a) Annual water budget across the MOPEX data set. Each point represents one year of a basin. The point colors represent different catchments. (b) Climatological, 50-year average, water balance from the MOPEX data set derived from the daily streamflow and precipitation data. Black continuous line is the Budyko curve and the dashed lines represent the +/−10% range of the Budyko curve. Basins where rainfall and potential evaporation are in phase (peaks within 3 months) are denoted with diamonds, Basins where rainfall and potential evaporation are out of phase (peaks within 6 months +/−2 months) are denoted with a square, the other basins are plotted with cross markers.

theoretical framework describing the optimal catchment vegetation based on a maximum soil moisture hypothesis. *Kerkhoff et al.* [2004] argued that this hypothesis could not be demonstrated based on observations since Eagleson's maximum soil moisture hypothesis is usually detrimental to species in their competition for light, water and nutrients with other species [*Caylor et al.*, 2006].

[6] To account for this vegetation dependence, Fu derived a parameterization for the Budyko curve with an added parameter accounting for vegetation that could shift the curve up and down [*Fu*, 1981]. *Potter et al.* [2005] however showed that in Summer-dominant rainfall, Fu's equation overestimated long-term evapotranspiration and that oppositely long-term evapotranspiration was under-estimated in Winter-dominant rainfall regimes. Instead most observed catchments had long-term evapotranspiration closer to the original non-parametric Budyko curve.

[7] Here, we take a view opposite to that of Fu: we assume that the Budyko curve holds across seasonality, soil and vegetation conditions and that it is only dependent on the annual aridity index. The unique long-term water balance across different catchments should reflect the interdependence among vegetation, soil and climate. The objective of this manuscript is to demonstrate the role of vegetation adaptation on the long-term hydrologic cycle in order to satisfy the Budyko relationship. The Budyko curve is inverted to yield insights into both above- and below-ground vegetation adaptations to soil and climate conditions.

2. The Budyko Curve as a Climatology

[8] We first want to stress that the Budyko curve only applies to the long-term water balance and neither to the annual nor interannual water balance. To this end, long-term (50 years) observed records of hourly precipitation, daily streamflow and potential evaporation from 431 catchments from the Model Parameter Estimation Experiment (MOPEX) [*Duan et al.*, 2006] located across the continental United States are used, spanning a wide range of ecological, soil and climate conditions. The drainage areas of the catchments vary between 67 and 10,329 km^2, and the data set is limited to catchments where interbasin groundwater flows are negligible. The E_p climatology for these catchments is based on NOAA's free water surface evaporation atlas [*Farnsworth et al.*, 1982]. Since the interannual variability in E_p is small [*Koster and Suarez*, 1999], approximately an order of magnitude smaller than that of precipitation, it is not accounted for in this study. Daily potential evaporation is thus computed as the interpolation of the monthly climatological values. We exclude those basins with missing data; records shorter than 50 years; significant topographical gradients, i.e., elevation changes greater than 1000m or slope steeper than 15 percent, since these basins are likely to span distinct climate regimes and associated impacts on the hydrologic cycle; important anthropogenic modifications (e.g., irrigation, reservoirs) based on the estimates of *Wang and Hejazi* [2011]. A total of 77 basins was removed from the analysis.

[9] Figure 1a depicts the relationship between annual $\overline{ET}/\overline{P}$ and the aridity index $\bar{\phi}$. Each point represents the annual data for one basin. Each color represents a different basin. The substantial spread across the data points implies distinct annual water budgets [*Yang et al.*, 2007; *Gerrits et al.*, 2009] and/or significant interannual storage changes. Nonetheless the Budyko curve has been incorrectly applied in many studies as a constraint on the annual and interannual water balance. In his original derivation Budyko only investigated the long-term water balance (over several decades).

[10] Figure 1b depicts the long-term – climatological - water balance for the same catchments. When using the climatological values, the dataset produces a much better fit to the Budyko curve than the annual values and 96% of the points fall within a 10% range of the Budyko curve (continuous black line). This 10% range is well within observational errors in precipitation and streamflow estimates at the catchment scale [*Potter et al.*, 2005]. The seasonality between rainfall and potential evaporation does not alter the fit of the basins to the Budyko curve. Noticeably, no systematic biases are present for summer or

winter-dominated rainfall regimes (Figure 1b). There are, however, departures from the curve in the most arid catchments, possibly a reflection of the effect of strong interannual vegetation variations in arid regions [*Donohue et al.*, 2007, 2010].

3. Inverting the Budyko Curve: Vegetation Adaptation

[11] To yield insights into the coupling between the soil, vegetation and climatic conditions, we use a typical soil bucket model [*Manabe* 1969; *Eagleson*, 1978a, 1978b, 1978c; *Rodríguez-Iturbe et al.*, 1999; *Laio et al.*, 2001]. The soil moisture budget is:

$$nz_r \frac{ds}{dt} = I(s) - L(s) - ET(s), \tag{2}$$

with n the soil porosity, s the relative soil moisture, z_r the volume of soil exploited by the roots per unit area. z_r scales as a distance and in the case of a dense canopy represents the rooting depth. In the case of the sparse canopies typical arid and semiarid environments the soil volume exploited by plants roots expands laterally; in this case z_r represents both the vertical rooting depth and lateral spread of the roots over the bare soil region. z_r will be called rooting distance in the rest of the manuscript for simplicity yet it represents an effective radius of influence of the roots that can be either vertical or horizontal. $I(s)$ is the soil infiltration, which is partitioned into a bare soil component, equal to the net precipitation rate minus infiltration excess runoff, and a vegetated component, where canopy rainfall interception r_i reduces the net precipitation rate. Infiltration excess runoff, which is important in semi-arid regions, is computed using a time-compression representation [*Salvucci and Entekhabi*, 1994; *Rigby and Porporato*, 2006; *Manfreda et al.*, 2010]. $L(s)$ is the leakeage, modeled as $k_{sat}s^c$ [*Brooks and Corey*, 1964] where k_{sat} is the saturation hydraulic conductivity and c is the shape parameter. Evapotranspiration is divided into a vegetated and bare-soil component as:

[12] $ET(s) = veg\ f_c E_p f_{\mathrm{veg}}(s) + (1 - veg)E_p f_{\mathrm{soil}}(s)$ (following *Eagleson* [1978b]), where *veg* is the vegetation fraction (between 0 and 1). The vegetation water stress $f_{veg}(s)$ is assumed to be piecewise linear $f_{veg}(s) = \max\left(\min\left(\frac{s - s_{wilt}}{s_* - s_{wilt}}, 1\right), 0\right)$, with s_{wilt} the soil moisture at the wilting point and s_* the soil moisture at which plants start to close stomata [*Manabe* 1969; *Porporato et al.*, 2002] and similarly the soil water stress is $f_{soil}(s) = \max\left(\min\left(\frac{s - s_{res}}{s_{fc} - s_{res}}, 1\right), 0\right)$ with s_{res} the residual soil moisture and s_{fc} the soil moisture at field capacity. The soil moisture parameters are related to the corresponding soil matric potentials through soil water retention curves (as in *Porporato et al.* [2002]). f_c is a dimensionless canopy transpiration efficiency representing the effect of the maximum transpiration achievable at the ecosystem scale [*Eagleson*, 1978b], which is equivalent to a crop coefficient, excluding the water stress computed in f_{veg} [*Allen et al.*, 1998].

[13] We here account for vegetation seasonality (*veg*) using the monthly climatological vegetation fractional cover of the MOPEX dataset based on NDVI. Snowfall is not dissociated from rainfall since potential evaporation is very small in winter. The few weeks of phase lag induced by snowmelt has negligible influence on the mean-annual hydrologic budget. Notice that equation (2) is meant to describe plot-scale soil water balance in conditions of negligible topographic effects, while the analysis presented in this paper is at the basin scale. Equation (2) does not account for topography, which is expected to modify the soil water balance (hence soil moisture controls on evapotranspiration) only in regions affected by conspicuous overland flow or by subsurface flow parallel to the slope. The overall dependence of water loss (combined ET, drainage, and runoff) on soil moisture embodied in these simplified bucket models (approximately linear for dry soils, flat for moderately wet soil, and highly concave upwards for wet soil) has been experimentally verified at a range of sites using conditionally-averaged precipitation and soil moisture data [*Salvucci*, 2001; *Sun et al.*, 2011].

[14] The model is forced with daily potential evaporation, which is sufficient to resolve the daily dynamics of soil moisture drying [*Rodríguez-Iturbe et al.*, 2001]. Hourly precipitation is used since convective rainfall affects runoff on hourly time scales, especially in semi-arid and arid regions [*Pilgrim et al.*, 1988]. The annual observed catchment evapotranspiration $\overline{ET_{obs}}$ is estimated as the residual of the precipitation $\overline{P}$ minus streamflow $\overline{Q}$.

[15] The Budyko curve (1) constrains the range of parameters of the soil water budget (2) since both equations hold true over climatological time scales. An interdependence of the climate (aridity index and seasonality), soil and vegetation parameters is thus imposed by the Budyko curve:

$$f(\text{climate}, \text{soil}, \text{vegetation}) = 0. \tag{3}$$

[16] In other words, assuming the validity of the Budyko relation, surface parameters can be constrained, as discussed below, such that the integrated water balance (2) best fits the Budyko curve (1). Figure 1b shows that there is no effect of seasonality on the Budyko curve, however seasonality should affect the water budget partitioning in (2). The only way the Budyko curve can hold across seasonality (here defined as the time lag between the peak in potential evaporation and the peak in rainfall τ, in months) is through soil and vegetation adaptation that modify the water partitioning in (2). In other words, for the aridity index and seasonality of a given catchment, the soil and vegetation parameters are constrained to fit the climatological Budyko curve:

$$f_{[\bar{\phi}],\tau}(k_{sat}, c; f_c, z_r, r_i, veg) = 0. \tag{4}$$

where r_i is the canopy interception. The MOPEX dataset provides estimates of the soil characteristics k_{sat} and c as calibrated for the NOAH model as well as the *veg* fraction seasonality. Thus for those observed conditions, the relationship (4) can be further constrained to the conditional functional:

$$f_{[\bar{\phi}],\tau,k_{sat},c,veg}(f_c, z_r, r_i) = 0, \tag{5}$$

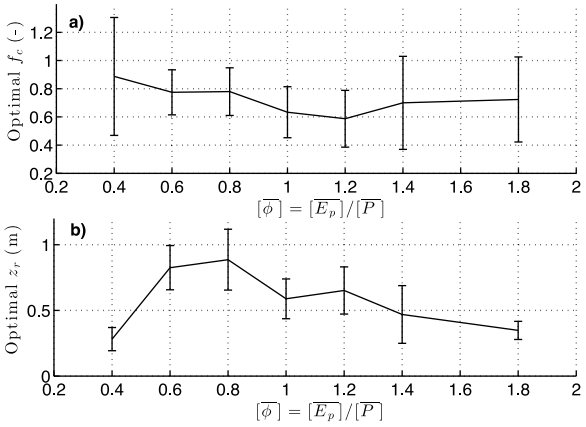

Figure 2. (a) Mean transpiration efficiency and (b) rooting distance obtained by the inversion of the Budyko curve, as a function of the aridity index. The mean and standard deviation are obtained by averaging the catchment values lying within the aridity index increment. In Figure 2a, the decreasing trend for aridity indices between 0.4 and 1.2 and the increasing trend above 1.2 are significant at the 5% level. In Figure 2b, the increasing trend for aridity indices between 0.4 and 0.8 and the decreasing trend above 0.8 are significant at the 5% level.

which emphasizes the coupling between belowground and aboveground vegetation structure. The transpiration efficiency f_c limits the transpiration and therefore carbon assimilation. In turn carbon is either allocated to aboveground canopy or belowground rooting system z_r, depending on the plant strategy.

[17] The possible multiple equilibria between rooting distance, rainfall interception and transpiration efficiency in equation (5) reflect the biodiversity for the particular climate and soil conditions. Reduction of the mismatch between modeled and observed interannual variability further discriminate between the multiple equlibria. The climatological Budyko curve constraint, condition (1), together with the match to interannual streamflow variability leads to an optimal solution of the triplet (f_c, z_r, r_i), reflecting the aggregated vegetation characteristics of the considered catchment. The optimal triplet is found by varying all parameters with one percent increments across the range of possible values. The global optimum is selected as the triplet with climatological ET falling within a 1% threshold of the Budyko curve and minimizing the annual streamflow error across all recorded years. The global optimum parameter triplet yields annual streamflow predictions with little error, i.e., root mean square errors of approximately 5% to 10% of the annual streamflow (25 to 140 mm). Increasing the threshold to the Budyko curve does not significantly alter the results presented here.

[18] Figure 2 depicts the optimal rooting distance and transpiration efficiency as a function of the climatological aridity index across the MOPEX catchments. The most humid catchments have shorter rooting distance compared to relatively water limited catchments (aridity index between 1 and 1.5) [*Laio et al.*, 2006] consistent with observations of increased lateral rooting spread in semi-arid regions to compensate for the small rainfall infiltration. In the driest basins (aridity index above 1.5), the rooting distance decreases again sharply, consistent with rooting depth observations along the Kalahari rainfall gradient [*Bhattachan et al.*, 2012]. This decrease reflects the predominance of non-perennial species (e.g., grass), which do not invest their carbon into rooting distance but rather invest into rapid growth and seeding.

[19] The transpiration efficiency is high in the most humid catchments reflecting efficient energy use because such catchments are energy limited. In the driest catchments, the transpiration efficiency again increases on average.

[20] Figure 3 depicts the dependence of rooting distance and transpiration efficiency on the seasonality lag between energy (potential evaporation) and water (rainfall) availability τ. Plants in climates with opposite phase between energy and water availability (e.g., Mediterranean climate) exhibit a much deeper rooting structure in order to cope with water stress [*Schenk and Jackson*, 2002]. Yearly transpiration would be reduced for out-of-phase radiation and precipitation without plant adaptation [*Feng et al.*, 2012]. The deeper rooting system introduces a lag in the surface soil moisture as evident in equation (2). Deep rooting systems reduce runoff and deep percolation, thus compensating for the phase difference between radiation and precipitation. In climates with smaller lags between peak E_p and P, plants do not need to invest their carbon resources into deep rooting systems in order to cope with short-term dry spells. It should be stressed that the water balance does not explicitly account for carbon allocation; rather, it appears naturally as a constraint of the observed Budyko curve.

4. Summary and Conclusions

[21] In this study, we have shown that the long-term surface hydrologic cycle could be a reflection of multiple vegetation adaptations, in particular those that are sensitive to the catchment dryness index and to the seasonality of rainfall and

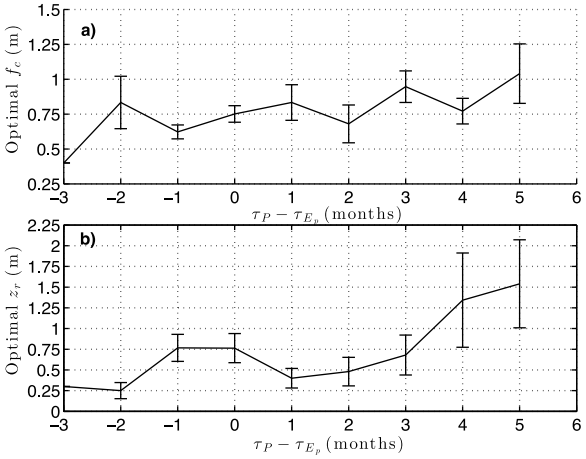

Figure 3. (a) Mean transpiration efficiency and (b) rooting distance resulting from the inversion of the Budyko curve, as a function of the phase between the peak in potential evaporation and precipitation τ. The gaps at 6, 7 and 8 months are due to insufficient data points. The mean and standard deviation are obtained by averaging the catchment values lying within the phase increment. In Figure 3a, the increasing trend is significant at the 5% level. In Figure 3b, the increasing trend above 1 month is significant at the 5% level.

radiation. Aboveground and belowground vegetation structures profoundly control the annual surface hydrological cycle and are both a cause and consequence of the surface water balance. We suggest that the fit of the modeled long-term surface water balance with the Budyko curve may provide a strong constraint on land-surface parameterizations in ungauged basins or general circulation models. The eco-hydrological insights from the inversion of the Budyko curve are tied to the land-surface, however our work demonstrates the potential strategies plants may employ to exert control on the annual surface water balance.

[22] **Acknowledgments.** The authors wish to than Peter Troch and Dingbao Wang for providing the datasets used in this work and for their feedback on our work. We also thank Fubao Sun, Amilcare Porporato and Peter Troch for their constructive criticism.

[23] The Editor thanks Peter Troch and an anonymous reviewer for assisting in the evaluation of this paper.

References

Allen, R. G., L. S. Pereira, D. Raes, and M. Smith (1998), Crop evapotranspiration—Guidelines for computing crop water requirements, *FAO Irrig. Drain. Pap. 56*, Food and Agric. Organ of the U. N., Rome.

Bhattachan, A., et al. (2012), Evaluating ecohydrological theories of woody root distribution in the Kalahari, *PLoS ONE*, *7*(3), e33996, doi:10.1371/journal.pone.0033996.

Brooks, R., and A. Corey (1964), Hydraulic properties of porous media, *Hydrol. Pap. 3*, Colo. State Univ., Fort Collins.

Budyko, M. (1961), *The Heat Balance of the Earth's Surface*, Natl. Weather Serv., U. S. Dep. of Commer., Washington, D. C.

Caylor, K. K., P. D'Odorico, and I. Rodríguez-Iturbe (2006), On the ecohydrology of structurally heterogeneous semiarid landscapes, *Water Resour. Res.*, *42*, W07424, doi:10.1029/2005WR004683.

Dietrich, W. E., and J. Perron (2006), The search for a topographic signature of life, *Nature*, *439*(7075), 411–418, doi:10.1038/nature04452.

Donohue, R. J., M. L. Roderick, and T. R. McVicar (2007), On the importance of including vegetation dynamics in Budyko's hydrological model, *Hydrol. Earth Syst. Sci.*, *11*(2), 983–995, doi:10.5194/hess-11-983-2007.

Donohue, R. J., M. L. Roderick, and T. R. McVicar (2010), Can dynamic vegetation information improve the accuracy of Budyko's hydrological model?, *J. Hydrol.*, *390*, 23–34, doi:10.1016/j.jhydrol.2010.06.025.

Duan, Q., et al. (2006), Model Parameter Estimation Experiment (MOPEX): An overview of science strategy and major results from the second and third workshops, *J. Hydrol.*, *320*, 3–17, doi:10.1016/j.jhydrol.2005.07.031.

Eagleson, P. S. (1978a), Climate, soil, and vegetation: 1. Introduction to water balance dynamics, *Water Resour. Res.*, *14*(5), 705–712, doi:10.1029/WR014i005p00705.

Eagleson, P. S. (1978b), Climate, soil, and vegetation: 2. The distribution of annual precipitation derived from observed storm sequences, *Water Resour. Res.*, *14*(5), 713–721, doi:10.1029/WR014i005p00713.

Eagleson, P. S. (1978c), Climate, soil, and vegetation: 3. A simplified model of soil moisture movement in the liquid phase, *Water Resour. Res.*, *14*(5), 722–730, doi:10.1029/WR014i005p00722.

Eagleson, P. (1982), Ecological optimality in water-limited natural soil-vegetation systems: 1. Theory and hypothesis, *Water Resour. Res.*, *18*(2), 325–340, doi:10.1029/WR018i002p00325.

Eagleson, P., and T. Tellers (1982), Ecological optimality in water-limited natural soil-vegetation systems: 2. Tests and applications, *Water Resour. Res.*, *18*(2), 341–354, doi:10.1029/WR018i002p00341.

Farnsworth, R. K., E. S. Thompson, and E. L. Peck (1982), Evaporation atlas for the contiguous 48 United States, *NOAA Tech. Rep. NWS 33*, 26 pp., NOAA, Washington, D. C.

Feng, X., G. Vico, and A. Porporato (2012), On the effects of seasonality on soil water balance and plant growth, *Water Resour. Res.*, *48*, W05543, doi:10.1029/2011WR011263.

Fu, B. P. (1981), On the calculation of the evaporation from land surface [in Chinese], *Chin. J. Atmos. Sci.*, *5*, 23–31.

Gerrits, A. M. J., H. H. G. Savenije, E. J. M. Veling, and L. Pfister (2009), Analytical derivation of the Budyko curve based on rainfall characteristics and a simple evaporation model, *Water Resour. Res.*, *45*, W04403, doi:10.1029/2008WR007308.

Horton, R. (1933), The role of infiltration in the hydrologic cycle, *Eos Trans. AGU*, *14*, 446–460.

Kerkhoff, A., S. Martens, and B. Milne (2004), An ecological evaluation of Eagleson's optimality hypotheses, *Funct. Ecol.*, *18*(3), 404–413, doi:10.1111/j.0269-8463.2004.00844.x.

Koster, R. D., and M. Suarez (1999), A simple framework for examining the interannual variability of land surface moisture fluxes, *J. Clim.*, *12*(7), 1911–1917, doi:10.1175/1520-0442(1999)012<1911:ASFFET>2.0.CO;2.

Laio, F., A. Porporato, L. Ridolfi, and I. Rodríguez-Iturbe (2001), Plants in water-controlled ecosystems: Active role in hydrologic processes and response to water stress—II. Probabilistic soil moisture dynamics, *Adv. Water Resour.*, *24*(7), 707–723, doi:10.1016/S0309-1708(01)00005-7.

Laio, F., P. D'Odorico, and L. Ridolfi (2006), An analytical model to relate vertical root distribution to climate and soil properties, *Geophys. Res. Lett.*, *33*, L18401, doi:10.1029/2006GL027331.

Manabe, S. (1969), Climate and ocean circulation. I. Atmospheric circulation and hydrology of the Earth's surface, *Mon. Weather Rev.*, *97*(11), 739–774, doi:10.1175/1520-0493(1969)097<0739:CATOC>2.3.CO;2.

Manfreda, S., T. M. Scanlon, and K. K. Caylor (2010), On the importance of accurate depiction of infiltration processes on modelled soil moisture and vegetation water stress, *Ecohydrology*, *3*, 155–165.

Milly, P. (1994), Climate, soil-water storage, and the average annual water-balance, *Water Resour. Res.*, *30*(7), 2143–2156, doi:10.1029/94WR00586.

Milly, P., and K. Dunne (2002), Macroscale water fluxes: 2. Water and energy supply control of their interannual variability, *Water Resour. Res.*, *38*(10), 1206, doi:10.1029/2001WR000760.

Ol'dekop, E. M. (1911), *On Evaporation From the Surface of River Basins*, Iur'evskogo Univ., Tartu, Estonia.

Pilgrim, D., T. Chapman, and D. Doran (1988), Problems of rainfall-runoff modeling in arid and semiarid regions, *Hydrol. Sci. J.*, *33*(4), 379–400, doi:10.1080/02626668809491261.

Porporato, A., P. D'Odorico, F. Laio, L. Ridolfi, and I. Rodríguez-Iturbe (2002), Ecohydrology of water-controlled ecosystems, *Adv. Water Resour.*, *25*(8–12), 1335–1348, doi:10.1016/S0309-1708(02)00058-1.

Porporato, A., E. Daly, and I. Rodríguez-Iturbe (2004), Soil water balance and ecosystem response to climate change, *Am. Nat.*, *164*(5), 625–632, doi:10.1086/424970.

Potter, N. J., L. Zhang, P. C. D. Milly, T. A. McMahon, and A. J. Jakeman (2005), Effects of rainfall seasonality and soil moisture capacity on mean annual water balance for Australian catchments, *Water Resour. Res.*, *41*, W06007, doi:10.1029/2004WR003697.

Rigby, J. R., and A. Porporato (2006), Simplified stochastic soil-moisture models: A look at infiltration, *Hydrol. Earth Syst. Sci.*, *10*(6), 861–871, doi:10.5194/hess-10-861-2006.

Rodríguez-Iturbe, I., A. Porporato, L. Ridolfi, V. Isham, and D. R. Cox (1999), Probabilistic modelling of water balance at a point: The role of climate, soil and vegetation, *Proc. R. Soc. A*, *455*, 3789–3805, doi:10.1098/rspa.1999.0477.

Rodríguez-Iturbe, I., A. Porporato, F. Laio, and L. Ridolfi (2001), Plants in water-controlled ecosystems: Active role in hydrologic processes and response to water stress—I. Scope and general outline, *Adv. Water Resour.*, *24*(7), 695–705, doi:10.1016/S0309-1708(01)00004-5.

Salvucci, G. D. (2001), Estimating the moisture dependence of root zone water loss using conditionally averaged precipitation, *Water Resour. Res.*, *37*(5), 1357–1365, doi:10.1029/2000WR900336.

Salvucci, G., and D. Entekhabi (1994), Equivalent steady soil-moisture profile and the time compression approximation in water-balance modeling, *Water Resour. Res.*, *30*(10), 2737–2749, doi:10.1029/94WR00948.

Schenk, H., and R. Jackson (2002), Rooting depths, lateral root spreads and below-ground/above-ground allometries of plants in water-limited ecosystems, *J. Ecol.*, *90*(3), 480–494, doi:10.1046/j.1365-2745.2002.00682.x.

Schreiber, P. (1904), Uber die Beziehungen zwischen dem Niederschlag und der Wasserfuhrung der Flusse in Mitteleuropa, *Z. Meteorol.*, *21*(10), 441–452.

Sivapalan, M., M. A. Yaeger, C. J. Harman, X. Xu, and P. A. Troch (2011), Functional model of water balance variability at the catchment scale: 1. Evidence of hydrologic similarity and space-time symmetry, *Water Resour. Res.*, *47*, W02522, doi:10.1029/2010WR009568.

Sun, J., G. D. Salvucci, D. Entekhabi, and L. Farhadi (2011), Parameter estimation of coupled water and energy balance models based on stationary constraints of surface states, *Water Resour. Res.*, *47*, W02512, doi:10.1029/2010WR009293.

Troch, P. A., et al. (2009), Climate and vegetation water use efficiency at catchment scales, *Hydrol. Processes*, *23*(16), 2409–2414, doi:10.1002/hyp.7358.

Wang, D., and M. Hejazi (2011), Quantifying the relative contribution of the climate and direct human impacts on mean annual streamflow in the contiguous United States, *Water Resour. Res.*, *47*, W00J12, doi:10.1029/2010WR010283.

Yang, D., F. Sun, Z. Liu, Z. Cong, G. Ni, and Z. Lei (2007), Analyzing spatial and temporal variability of annual water-energy balance in nonhumid

regions of China using the Budyko hypothesis, *Water Resour. Res.*, *43*, W04426, doi:10.1029/2006WR005224.

Yang, H., D. Yang, Z. Lei, and F. Sun (2008), New analytical derivation of the mean annual water-energy balance equation, *Water Resour. Res.*, *44*, W03410, doi:10.1029/2007WR006135.

Zhang, L., N. Potter, K. Hickel, Y. Zhang, and Q. Shao (2008), Water balance modeling over variable time scales based on the Budyko framework—Model development and testing, *J. Hydrol.*, *360*, 117–131, doi:10.1016/j.jhydrol.2008.07.021.